References

1 LONG, S.A., McALLISTER, M.W., and SHEN, L.C.: 'The resonant cylindrical dielectric cavity antenna', *IEEE Trans. Antennas Propag.*, 1983, **AP-31**, pp. 406–412

2 LEUNG, K.W., LUK, K.M., YUNG, E.K.N., and LAI, S.: 'Characteristics of a low-profile circular disk DR antenna with very high permittivity', *Electron. Lett.*, 1995, **31**, pp. 417–418

3 MONGIA, R.K., ITTIBIPOON, A., and CUHACI, M.: 'Low profile dielectric resonator antennas using a very high permittivity material', *Electron. Lett.*, 1994, **30**, pp. 1362–1363

4 LU, J.H., TANG, C.L., and WONG, K.L.: 'Single-feed slotted equilateral-triangular microstrip antenna for circular polarization', *IEEE Trans. Antennas Propag.*, 1999, **AP-47**, pp. 1174–1178

5 HASSANI, H.R., and MIRSHEKAR-SYAHKAL, D.: 'Analysis of triangular patch antennas including radome effects', *IEE Proc. H*, 1992, **139**, pp. 251–256

6 YOSHIHIKO, A.: 'Operation modes of a waveguide Y circulator', *IEEE Trans. Microw Theory Tech.*, 1974, **MTT-23**, pp. 954–960

Microstrip antenna-coupled infrared detector

I. Codreanu, C. Fumeaux, D.F. Spencer and G.D. Boreman

A novel type of antenna-coupled infrared detector consisting of a niobium microbolometer integrated with two microstrip patch antennas is reported. This is the first microstrip antenna structure proven to detect thermal infrared radiation. A polarisation ratio of > 20:1 and a time constant of < 150ns have been measured for this type of detector.

Introduction: Antenna-coupled infrared detectors achieve a fast response by separating the radiation collection and detection functions. They consist of an antenna and an electrical sensor (bolometer, metal-oxide-metal diode, etc.). In general, the antenna size is comparable to the wavelength of the radiation being detected, while the sensor is just a fraction of the wavelength to allow for a fast response. The antenna collects the radiation and supplies an electrical signal which is processed by the sensor. Integrated infrared detectors using dipole antennas [1], bowtie antennas [2, 3], log-periodic antennas [2], and spiral antennas [3, 4] have been reported.

Microstrip antennas are widely used in the microwave spectral region. They are easy to fabricate using standard integrated circuit techniques, have a low profile, are conformal, and can be easily integrated in arrays and with electronic components. Microstrip antennas produce broadside and narrowband radiation (at most a few percent of the centre frequency). A low gain is the major drawback of microstrip antennas. In general, the narrow bandwidth of the microstrip antenna is considered inconvenient, and various schemes have been devised to alleviate the problem. However, applications such as frequency tuning take advantage of the inherent narrow bandwidth of the microstrip antenna.

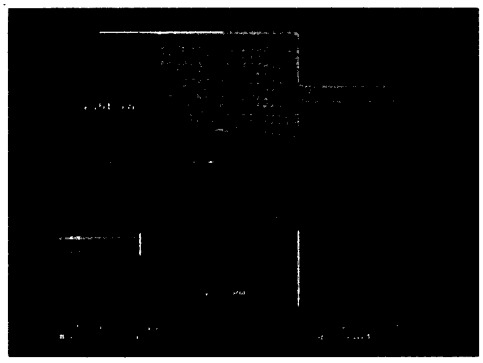

Fig. 1 *Electron micrograph of integrated detector*

Device: The device investigated is shown in Fig. 1. It consists of two rectangular microstrip antennas connected by a 70nm thick niobium bridge. Both the rectangular patches (100nm thick) and the ground plane (170nm thick) are made of gold. A 200nm thick silicon dioxide layer is employed as a dielectric substrate. The silicon dioxide was deposited by plasma enhanced chemical vapour deposition (PECVD), the antenna was electron beam evaporated, and the microbolometer was fabricated by sputtering. The metal parts were patterned by electron beam lithography and lift-off. The horizontal narrow lines seen in Fig. 1 on each side of the antennas are used as DC leads providing a bias and electrical readout for the bolometer.

Two 2.6μm long, 3.4μm wide patch antennas were fabricated. The antenna length, equal to about half the effective wavelength, determines the resonance; the width is chosen to achieve good radiation efficiency [5]. The antenna is designed to resonate at 10.6μm and be vertically polarised. Some response is also expected from the DC leads, but this should be just a few percent of the antenna response. The bolometer consists of a 1.5μm long, 350nm wide niobium strip.

The incident infrared radiation induces terahertz electrical currents in the gold patches and on the ground plane. Part of these currents flows from one patch to the other, through the bolometer. This current dissipates into the bolometer, heating it, and thus providing the detection mechanism.

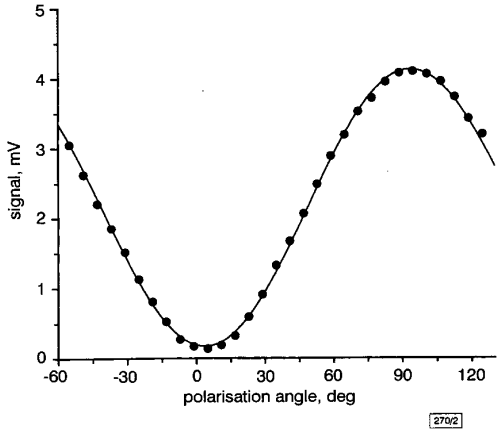

Fig. 2 *Polarisation dependence of detector response to 10.6μm radiation*

Maximum response angle is close to 90° and polarisation ratio is 23.6
● measured signal
——— cosine-squared fit

Results: The fabrication of these devices resulted in > 90% yield. The average electrical resistance of the detector is 205 ± 6Ω.

The detector was tested using linearly polarised 10.6μm carbon dioxide (CO_2) laser radiation focused with F/1 optics. The measurements showed that the detector is indeed vertically polarised (Fig. 2). The measured polarisation ratio, in excess of 20, is the highest reported for an antenna-coupled infrared detector [6].

Up to 200mV, the detector response is proportional to the bias voltage. The signal starts to saturate above 200mV, and device failure is induced for a bias voltage exceeding 500mV.

At low modulation frequencies the performance of the device is degraded by $1/f$ noise. Above 100kHz, the device is primarily Johnson noise limited. The detector response starts to roll over at 800kHz. Consequently, the optimal signal-to-noise (S/N) ratios are obtained in a range of modulation frequencies extending from 100 to 800kHz. The response of the microbolometers is extremely fast; a time constant of < 150ns has been measured for these devices.

To obtain the detector collection area, the 11μm radius CO_2 laser beam was scanned across the detector plane. The measured two-dimensional spatial response is a convolution of the detector spatial response with the irradiance distribution of the laser beam used to illuminate it. The detector spatial response is extracted using the approach reported in [7]. Fig. 3 shows the geometric structure of the antenna-coupled infrared detector along with the contours of the areas enclosing 50 and 90% of the volume of the spatial response. The 90% contour contains a 24μm² area and has a 2.2 axial ratio.

The power received by the antenna-coupled detector is determined from the collection area and the laser beam irradiance. Based on the collected power, we estimate a room-temperature noise-equivalent power (NEP) of < 7nW/Hz$^{1/2}$. This NEP is measured at an operating bias voltage of 100mV and at high frequency, where the Johnson noise dominates the $1/f$ noise. Optimisation of the resonance frequency of the antenna is expected to decrease this NEP.

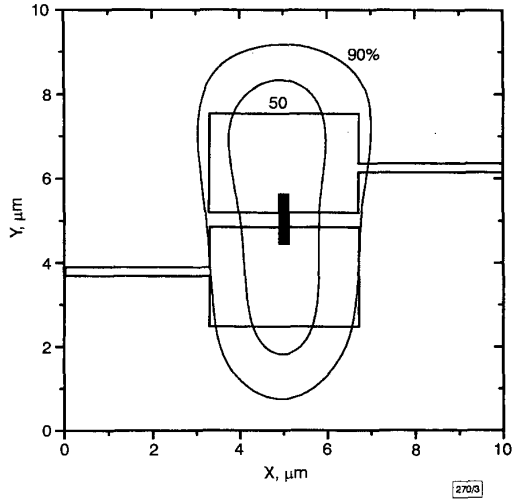

Fig. 3 *Geometry of antenna-coupled infrared detector*

Contours of areas enclosing 50 and 90% of volume of spatial response are shown

Conclusions: The first microstrip antenna structure that detects thermal infrared radiation has been reported. It has an excellent polarisation ratio (> 20:1), is extremely fast for a bolometer detector (150 ns), and has a collection area of 24μm^2. The NEP is of the order of 7nW/Hz$^{1/2}$.

Acknowledgment: The authors acknowledge the support of Lockheed-Martin Corporation and of the Ballistic Missile Defense Organisation

29 October 1999
Electronics Letters Online No: 19991486
DOI: 10.1049/el:19991486

I. Codreanu, C. Fumeaux and G.D. Boreman (*School of Optics/CREOL, University of Central Florida, 4000 Central Florida Blvd., Orlando, FL 32816, USA*)

E-mail: boreman@mail.creol.ucf.edu

D.F. Spencer (*CNF, Cornell University, G06 Knight Lab., Ithaca, NY 14853, USA*)

References

1 WILKE, I., HERRMANN, W., and KNEUBÜHL, F.K.: 'Integrated nanostrip dipole antennas for coherent 30THz infrared radiation', *Appl. Phys. B*, 1994, **58**, (2), pp. 87–95

2 CHONG, N., and AHMED, H.: 'Antenna-coupled polycrystalline silicon air-bridge thermal detector for mid-infrared radiation', *Appl. Phys. Lett.*, 1997, **71**, (12), pp. 1607–1609

3 FUMEAUX, C., HERRMANN, W., KNEUBÜHL, F.K., and ROTHUIZEN, H.: 'Nanometer thin-film Ni-NiO-Ni diodes for detection and mixing of 30THz radiation', *Infrared Phys. Technol.*, 1998, **39**, (3), pp. 123–183

4 GROSSMAN, E.N., SAUVAGEAU, J.E., and McDONALD, D.G.: 'Lithographic spiral antennas at short wavelengths', *Appl. Phys. Lett.*, 1991, **59**, (25), pp. 3225–3227

5 BALANIS, C.A.: 'Antenna theory: analysis and design' (John Wiley & Sons, New York, 1997), 2nd edn.

6 GROSSMAN, E.N., KOCH, J.A., REINTSEMA, C.D., and GREEN, A.: 'Lithographic dipole antenna properties at 10μm wavelength: comparison of method of moments predictions with experiment', *Int. J. Infrared Millim. Waves*, 1998, **19**, (6), pp. 817–825

7 ALDA, J., FUMEAUX, C., CODREANU, I., SCHAEFER, J.A., and BOREMAN, G.D.: 'Deconvolution method for two-dimensional spatial-response mapping of lithographic infrared antennas', *Appl. Opt.*, 1999, **38**, (19), pp. 3992–4000

Adaptive predistorter for power amplifier based on real-time estimation of envelope transfer characteristics

Jae-Hee Han, Tasik Chung and Sangwook Nam

A new adaptation technique for digital predistortion is presented. The proposed method employs the real-time input and output signals of a high power amplifier (HPA) to estimate the complex envelope transfer characteristics. Therefore, a look-up table update can be performed without interrupting the normal transmission of messages through an HPA.

Introduction: Spectral regrowth (SR) or intermodulation distortion (IMD) generated by a nonlinear high power amplifier (HPA) causes interferences in adjacent communication channels. Hence, many linearisation techniques for HPAs such as feedforward, feedback and predistortion have been developed to combat these problems. These linearisers should be adaptive to the variations in the characteristics of the HPA. The digital predistorter is one of the most promising means for carrying out linearisation because of its high levels of performance and adaptability [1 – 4].

In a digital predistorter, the input signals are distorted according to a look-up table (LUT) which contains the inverse characteristics of the HPA. To maintain the suppressed SR or IMD at a desired level, the LUT should be updated with the changes in the characteristics of the HPA [2]. Therefore, fast and precise adaptation is an important issue in digital predistortion because it determines the system performance.

In this Letter, a new adaptation technique for the digital predistorter is proposed. The LUT is updated by the real-time estimation of the complex envelope transfer characteristics of the HPA. The estimation is carried out using the real signals transmitted through the HPA. Moreover, the proposed estimation algorithm does not depend on the modulation format.

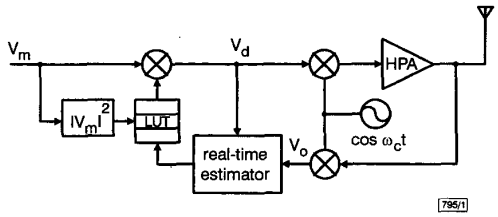

Fig. 1 *Simplified block diagram of proposed digital predistorter*

Description of system: A simplified block diagram of the proposed system is shown in Fig. 1. This system is composed of the predistorter and the estimator. In the predistortion part, the desired signal V_m is distorted according to a one-dimensional LUT [2] and applied to the input of the HPA. In the estimation part, the input and output complex envelopes of the HPA, V_d and V_o, are sampled for the real-time estimation of the complex envelope transfer function. Its inverse function is then obtained to be used to update the LUT. The flowchart for the entire estimation and update procedure is shown in Fig. 2.

Estimation of characteristics: Using the notation in Fig. 1, the relationship between the input and output complex envelope of the HPA can be expressed by [1]

$$V_o = \sum_{k=0}^{N} \beta_{k+1} r_d^{2k} V_d \qquad (1)$$

where $r_d = |V_d| = \sqrt{[I_d^2 + Q_d^2]}$ and the complex coefficients $\beta_k = a_k + jb_k$ account for the AM/AM and AM/PM distortions of the HPA. Taking the real part of eqn. 1, the output in-phase component becomes